



# Symmetric Union Diagrams and Refined Spin Models

Carlo Collari and Paolo Lisca

*Abstract.* An open question akin to the slice-ribbon conjecture asks whether every ribbon knot can be represented as a symmetric union. Next to this basic existence question sits the question of uniqueness of such representations. Eisermann and Lamm investigated the latter question by introducing a notion of symmetric equivalence among symmetric union diagrams and showing that non-equivalent diagrams can be detected using a refined version of the Jones polynomial. We prove that every topological spin model gives rise to many effective invariants of symmetric equivalence, which can be used to distinguish infinitely many Reidemeister equivalent but symmetrically non-equivalent symmetric union diagrams. We also show that such invariants are not equivalent to the refined Jones polynomial and we use them to provide a partial answer to a question left open by Eisermann and Lamm.

## 1 Introduction

### 1.1 Symmetric Diagrams and Symmetric Equivalences

Let  $\rho: \mathbb{R}^2 \rightarrow \mathbb{R}^2$  be the reflection given by  $\rho(x, y) = (-x, y)$ . The map  $\rho$  fixes pointwise the subset  $B = \{0\} \times \mathbb{R} \subset \mathbb{R}^2$ , which will be called the *axis*. Two diagrams  $D, D' \subset \mathbb{R}^2$  will be considered identical if there is an orientation-preserving diffeomorphism  $h: \mathbb{R}^2 \rightarrow \mathbb{R}^2$  such that  $h \circ \rho = \rho \circ h$  and  $h(D) = D'$ .

An oriented link diagram  $D \subset \mathbb{R}^2$  is *symmetric* if  $\rho(D) = \bar{D}$ , where  $\bar{D}$  is the oriented diagram obtained from  $D$  by reversing the orientation and switching all the crossings on the axis. A symmetric diagram  $D$  is a *symmetric union* if  $\rho$  sends each component  $c_D$  of  $D$  to itself in an orientation-reversing fashion, implying that  $c_D$  crosses the axis perpendicularly in exactly two non-crossing points. Figure 1 shows two unoriented symmetric union diagrams of the amphicheiral knot  $8_9$ . The two diagrams are obtained from each other by switching all the crossings on the axis, which amounts to reflecting across the plane of the page and then applying a 3-dimensional  $180^\circ$  rotation around the axis. Eisermann and Lamm [3, §2.4] observed that with each symmetric diagram one can associate a singular link  $L \subset \mathbb{R}^3$  with some extra data. This is done by converting each crossing on the axis into a double point belonging to the plane  $E = \{x = 0\} \subset \mathbb{R}^3$  and by encoding the over-under crossing information by a sign attached to the double point according to the rules of Figure 2. The resulting singular link with signs, transverse to  $E$  and invariant under reflection with respect to  $E$ , is what we call a *symmetric singular link*. We say that two symmetric

---

Received by the editors June 23, 2018; revised October 29, 2018.

Published online on Cambridge Core March 25, 2019.

The first author was partially supported by an Indam grant, and hosted by the IMT in Toulouse, during the early stages of this paper.

AMS subject classification: 57M27, 57M25.

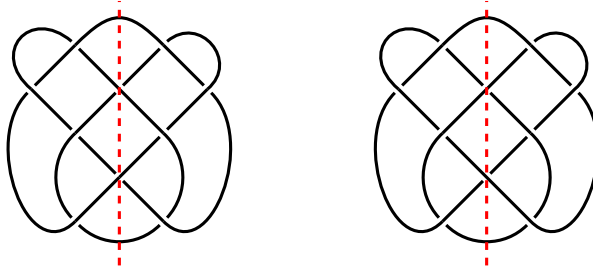


Figure 1: (Colour online) Symmetric union diagrams of the knot  $8_9$ .



Figure 2: (Colour online) How to turn a crossing on the axis into a signed double point.

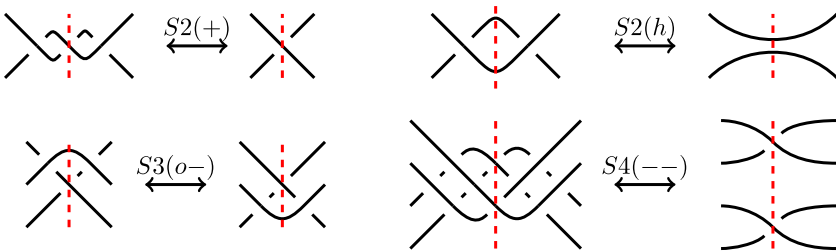


Figure 3: (Colour online) Representative symmetric Reidemeister moves.

diagrams are *strongly symmetrically equivalent* if their associated symmetric singular links can be connected via a smooth family of symmetric singular links. Eisermann and Lamm [3, Theorem 2.12] showed that symmetric diagrams satisfy a symmetric version of the Reidemeister theorem, where the symmetric analogues of the Reidemeister moves relating two symmetric diagrams are defined as follows.

A *symmetric Reidemeister move off the axis* is an ordinary Reidemeister move carried out, away from the axis  $B$ , together with its mirror-symmetric counterpart with respect to  $B$ . A *symmetric Reidemeister move on the axis* is one of the moves  $S2(h)$ ,  $S2(\pm)$ ,  $S3(o\pm)$ ,  $S3(u\pm)$ , and  $S4(\pm\pm)$ , some of which are illustrated in Figure 3 (see [3, §2.3] for the complete list). It is understood that these moves admit variants obtained by turning the corresponding pictures upside down, mirroring or rotating them around the axis. With our present terminology, Eisermann and Lamm proved the following.

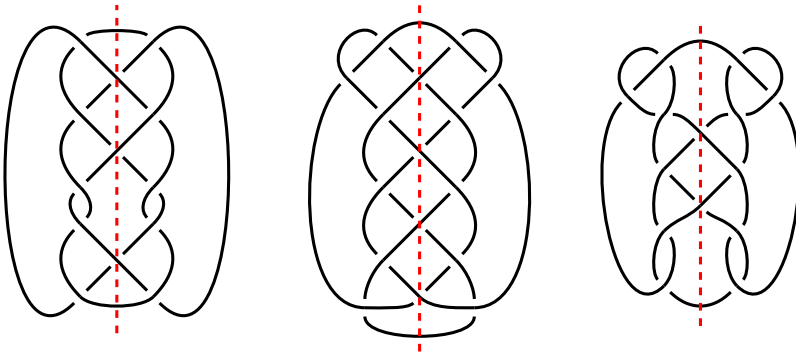


Figure 4: (Colour online) Symmetric union diagrams of  $8_9$  (left) and  $10_{42}$  (center and right).

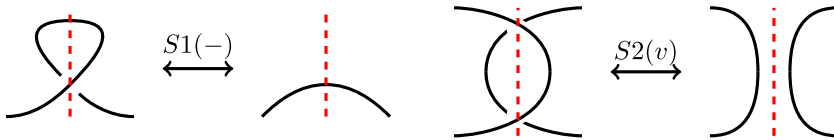


Figure 5: Extra moves  $S1(-)$  and  $S2(v)$ .

**Theorem 1.1** (Symmetric Reidemeister Theorem [3, Theorem 2.12]) *Two symmetric diagrams are strongly symmetrically equivalent if and only if they can be obtained from each other via a finite sequence of symmetric Reidemeister moves.*<sup>1</sup>

Eisermann and Lamm showed [3, Example 6.8] that the two symmetric union diagrams of the knot  $8_9$  given in Figure 1 are strongly symmetrically equivalent. On the other hand, they also consider another symmetric union diagram for the knot  $8_9$ , i.e., the left-most diagram of Figure 4, as well as the center and right-most diagrams in Figure 4, which are two symmetric union diagrams for the knot  $10_{42}$ . The two symmetric union diagrams of  $10_{42}$  in Figure 4 are not strongly symmetrically equivalent, because the associated symmetric singular links have different numbers of double points (four and two). Similarly, the symmetric union diagram of  $8_9$  from Figure 4 is not strongly symmetrically equivalent to the diagram of the same knot obtained by switching all the crossings on the axis, because the two diagrams have different numbers of signed crossings on the axis. (Note that both diagrams represent  $8_9$  because they clearly represent mirror equivalent knots, and  $8_9$  is amphicheiral).

These examples show that the notion of strong symmetric equivalence is not a very subtle one, but Eisermann and Lamm considered two extra moves on symmetric diagrams, which they called  $S1(\pm)$  and  $S2(v)$ . Some examples of the extra moves are illustrated in Figure 5.

<sup>1</sup>Eisermann and Lamm stated only one of the two implications of Theorem 1.1, but they used a terminology slightly different from ours and they included the moves  $S1$  and  $S2(v)$  of Figure 5 among their symmetric Reidemeister moves. It can be easily checked that in our terminology and for the set of moves of Figure 3, Theorem 2.12 from [3] is equivalent to Theorem 1.1 (see [3, Remark 2.13]).

**Definitions 1.2** Two oriented, symmetric diagrams that can be obtained from each other via a finite sequence of symmetric Reidemeister (or *sR*) moves and S1 moves will be called *symmetrically equivalent*. If they can be obtained from each other using *sR* moves, S1 moves, and  $S2(\nu)$  moves, we will say that the diagrams are *weakly symmetrically equivalent*.

The notions of symmetric equivalence introduced with Definitions 1.2 are more subtle than strong symmetric equivalence: for instance, it is not obvious whether the two symmetric diagrams of  $8_9$  and  $10_{42}$  described above are symmetrically equivalent (weakly or not).

### 1.2 Eisermann and Lamm’s Refined Jones Polynomial and Its Applications

With each oriented link diagram  $D \subset \mathbb{R}^2$  transverse to  $B = \{0\} \times \mathbb{R}$ , Eisermann and Lamm associated an invariant of weak symmetric equivalence  $W(D)$  taking values in the quotient field  $\mathbb{Z}(X_A, X_B)$  of the ring of Laurent polynomials in the variables  $X_A$  and  $X_B$  with integer coefficients. The invariant is defined by setting  $W(D) = (-X_A^{-3})^{w_A(D)}(-X_B^{-3})^{w_B(D)}\langle D \rangle$ , where  $w_A(D)$  and  $w_B(D)$  are, respectively, the sum of crossing signs off and on the axis, and  $\langle D \rangle$  is a refined Kauffman bracket specified by the skein relation

$$\langle \text{crossing off axis} \rangle = X_A \langle \text{cup} \rangle + X_A^{-1} \langle \text{cap} \rangle$$

for crossings off the axis, the skein relations

$$\begin{aligned} \langle \text{crossing on axis} \rangle &= X_B \langle \text{cup} \rangle + X_B^{-1} \langle \text{cap} \rangle, \\ \langle \text{crossing on axis} \rangle &= X_B^{-1} \langle \text{cup} \rangle + X_B \langle \text{cap} \rangle \end{aligned}$$

for crossings on the axis, and taking the value

$$\langle C \rangle = (-X_A^2 - X_A^{-2})^{n-m}(-X_B^2 - X_B^{-2})^{m-1}$$

on a collection  $C$  of  $n$  circles intersecting the axis  $B$  in  $2m$  points.

It turns out [3, Propostion 1.8] that when  $D$  is a symmetric union knot diagram, the invariant  $W(D)$  is an honest Laurent polynomial. Using the  $W$ -polynomial, Eisermann and Lamm showed in [3] that the diagram for  $8_9$  in Figure 4 is not weakly symmetrically equivalent to the one obtained by switching crossings on the axis, and they exhibit an infinite family of pairs of symmetric union 2-bridge knot diagrams  $(D_n, D'_n)$  such that  $D_n$  and  $D'_n$  are Reidemeister equivalent but not weakly symmetrically equivalent for  $n = 3$  and  $n \geq 5$ . The diagrams  $D_4$  and  $D'_4$ , representing the knot  $10_{42}$ , are those shown in Figure 4. They have the same  $W$ -polynomial, so the question of their (weak) symmetric equivalence was left unanswered.

### 1.3 Results and Contents of the Paper

Our main result is Theorem 2.5, stating that (i) every topological spin model [6] gives rise to infinitely many invariants of symmetric equivalence and (ii) such invariants

satisfying a certain extra condition are in fact invariants of weak symmetric equivalence. As we point out in Remark 2.4, each topological spin model gives rise in this way to at least four (essentially equivalent) invariants of weak symmetric equivalence.

We give the following three applications of Theorem 2.5.

(1) Let  $D_{10_{42}}$  (respectively,  $D'_{10_{42}}$ ) be the central (respectively the right-most) symmetric union diagram of Figure 4. We prove that  $D_{10_{42}}$  and  $D'_{10_{42}}$  are not symmetrically equivalent, providing a partial answer to a question left open by Eisermann and Lamm [3, §6.4].

(2) Let  $D_{8_9}$  be the left-most diagram of Figure 4, and let  $D'_8$  be the diagram obtained from  $D_{8_9}$  by switching all the crossings on the axis. As we explained in the paragraph immediately following Theorem 1.1, the two diagrams  $D_{8_9}$  and  $D'_8$  are Reidemeister equivalent. We use Theorem 2.4 to prove that  $D_{8_9}$  and  $D'_8$  are not weakly symmetrically equivalent.

(3) We apply a gluing formula in conjunction with Theorem 2.5 to construct, for each  $n \geq 1$ , symmetrically non-equivalent symmetric union diagrams of the connected sum of  $n$  copies of  $10_{42}$ , as well as weakly symmetrically non-equivalent symmetric union diagrams of the connected sum of  $n$  copies of  $8_9$ .

Section 2 contains the necessary background material and the statement of Theorem 2.5. Section 3 contains the proof of Theorem 2.5. Section 4 contains three applications of Theorem 2.5, and Section 5 the proof of the gluing formula.

## 2 Spin Models and Their Refinements

### 2.1 Spin Models

We recall the theory of topological spin models for links in  $S^3$  as introduced in [6]. Let  $X = \{1, 2, \dots, n\}$ ,  $n \geq 2$ , denote by  $\text{Mat}_X(\mathbb{C})$  the space of square  $n \times n$  complex matrices whose rows and columns are indexed by elements of the set  $X$ , and let  $d \in \{\pm\sqrt{n}\}$ . Given a symmetric, complex matrix  $W^+ \in \text{Mat}_X(\mathbb{C})$  with non-zero entries, let  $W^- \in \text{Mat}_X(\mathbb{C})$  be the matrix uniquely determined by the equation

$$(2.1) \quad W^+ \circ W^- = J,$$

where  $\circ$  is the Hadamard, *i.e.*, entry-wise, product and  $J$  is the all-1 matrix. Define, for each matrix  $A \in \text{Mat}_X(\mathbb{C})$  with non-zero entries and  $a, b \in X$ , the vector  $Y_{ab}^A \in \mathbb{C}^X$  by setting

$$Y_{ab}^A(x) := \frac{A(x, a)}{A(x, b)} \in \mathbb{C}, \quad x \in X.$$

Then the pair  $M = (W^+, d)$  is a *spin model* if the following equations hold:

$$(2.2) \quad W^+ Y_{ab}^{W^+} = d W^-(a, b) Y_{ab}^{W^+} \quad \text{for every } a, b \in X.$$

Observe that, since  $Y_{aa}^{W^+}$  is the all-1 vector for each  $a \in X$ , taking  $b = a$  in equation (2.2) gives

$$(2.3) \quad \frac{1}{d} \sum_{x \in X} W^+(y, x) = W^-(a, a) \quad \text{for every } y, a \in X.$$

In particular,  $W^-(a, a)$  and therefore the *modulus*

$$\alpha_W = W^+(a, a) = 1/W^-(a, a) \in \mathbb{C}$$

of the spin model, are independent of  $a \in X$ .

**Examples 2.1** (1) Let  $n \geq 2$  be an integer and  $d \in \{\pm\sqrt{n}\}$ . Let  $\xi \in \mathbb{C} \setminus \{0\}$  be one of the four complex numbers such that  $d = -\xi^2 - \xi^{-2}$ . Then, setting  $W_{\text{Potts}}^+ = (-\xi^{-3})I + \xi(J - I)$ , the pair  $(W_{\text{Potts}}^+, d)$  is the well-known *Potts model* introduced in [6].

(2) Let  $d = \sqrt{5}$ ,  $\omega = e^{2\pi i/5}$ , and

$$W_{\text{pent}}^+ = \begin{pmatrix} 1 & \omega & \omega^{-1} & \omega^{-1} & \omega \\ \omega & 1 & \omega & \omega^{-1} & \omega^{-1} \\ \omega^{-1} & \omega & 1 & \omega & \omega^{-1} \\ \omega^{-1} & \omega^{-1} & \omega & 1 & \omega \\ \omega & \omega^{-1} & \omega^{-1} & \omega & 1 \end{pmatrix}.$$

Then  $(W_{\text{pent}}^+, d)$  is one of the spin models studied in [4] and mentioned in [6, 7]. We shall call it the *pentagonal model*, like the rescaled version  $(-iW_{\text{pent}}^+, -\sqrt{5})$  considered in [1].

A spin model  $M = (W^+, d)$  defines a link invariant as follows. Let  $D \subset \mathbb{R}^2$  be a connected diagram of an oriented link. Let  $\Gamma_D$  be the planar, signed medial graph associated with the black regions of any checkerboard colouring of  $\mathbb{R}^2 \setminus D$ . Let  $\Gamma_D^0$ ,  $\Gamma_D^1$  be the sets of vertices, respectively, edges of  $\Gamma_D$ , and let  $N = |\Gamma_D^0|$ . Given  $e \in \Gamma^1$ , we denote by  $v_e$  and  $w_e$  (in any order) the vertices of  $e$ . Define the *partition function*  $Z_M(D) \in \mathbb{C}$  by

$$Z_M(D) = d^{-N} \sum_{\sigma: \Gamma_D^0 \rightarrow X} \prod_{e \in \Gamma_D^1} W^{s(e)}(\sigma(v_e), \sigma(w_e)),$$

where the sum is taken over the set of all maps  $\sigma$  from  $\Gamma_D^0$  to  $X$ , and  $s(e) \in \{+, -\}$  is the sign of the edge  $e$ . Let the *normalized partition function*  $I_M(D)$  be  $I_M(D) := \alpha_W^{-w(D)} Z_M(D)$ , where  $w(D)$  is the writhe of  $D$ . When  $D$  is not connected, we define both  $Z_M(D)$  and  $I_M(D)$  as the product of the values of  $Z_M$  and, respectively,  $I_M$ , on its connected components.

**Theorem 2.2** ([6]) *Let  $M = (W^+, d)$  be a spin model and  $D \subset \mathbb{R}^2$  a connected, oriented link diagram. Then we have the following.*

- (i)  $I_M(D)$  is independent of the choice of colouring,
- (ii)  $I_M(D) = I_M(D')$  for every link diagram  $D'$  Reidemeister equivalent to  $D$ .

### 2.2 Refined Spin Models

Our idea is to refine the definition of a topological spin model by taking into account the presence of the axis, in the spirit of the refined Jones polynomial of Subsection 1.2. Let  $D \subset \mathbb{R}^2$  be an oriented link diagram transverse to the axis  $B = \{0\} \times \mathbb{R}$ . Since  $B$  goes through some of the crossings of  $D$ , for any choice of a checkerboard colouring

of  $\mathbb{R}^2 \setminus D$ , the corresponding medial graph  $\Gamma_D$  acquires some distinguished edges. We will assign suitably chosen weights to such distinguished edges.

Let  $X = \{1, \dots, n\}$  with  $n \geq 2$ , and let  $(W^+, d)$  be a spin model with  $W^+ \in \text{Mat}_X(\mathbb{C})$ . Recall from Subsection 2.1 that the matrix  $W^+$  determines the vectors  $Y_{ab}^W \in \mathbb{C}^X$ ,  $a, b \in X$ . Nomura [8] showed that the set  $N_W \subset \text{Mat}_X(\mathbb{C})$  of matrices that have the vectors  $Y_{ab}^W$  as eigenvectors is a commutative algebra with respect to both the ordinary matrix product and the Hadamard product. Sometimes  $N_W$  is called the *Nomura algebra*. Clearly, equation (2.2) implies  $W^+ \in N_W$ . Let  $\psi: N_W \rightarrow \text{Mat}_X(\mathbb{C})$  be the map defined by requiring that, for each  $A \in N_W$ , the matrix  $\psi(A)$  satisfies

$$AY_{ab}^{W^+} = \psi(A)(a, b)Y_{ab}^{W^+} \quad \text{for every } a, b \in X.$$

We will use the following facts: (1)  $N_W$  is closed under transposition and (2)  $N_W$  is *self-dual*, which means that  $\psi$  induces a linear isomorphism  $\psi: N_W \rightarrow N_W$  and  $\psi^2 = n\tau$ , where  $\tau: N_W \rightarrow N_W$  is the transposition map. For these facts, as well as for more information about the Nomura algebra, we refer the reader to [5]. Observe that equation (2.2) is equivalent to the equality  $W^- = \psi(W^+)/d$ , hence  $W^- \in N_W$ . More generally, given any matrix  $A^+ \in N_W$ , we can define  $A^- := \psi(A^+)/d \in N_W$ . Then it follows from  $\psi^2 = n\tau$  and  $d^2 = n$  that  $A^+ = \psi(A^-)/d$ . In the same way as equation (2.3) we deduce, for every  $y, a \in X$ ,

$$(2.4) \quad \frac{1}{d} \sum_{x \in X} A^+(y, x) = A^-(a, a), \quad \frac{1}{d} \sum_{x \in X} A^-(y, x) = A^+(a, a).$$

In particular, the complex numbers  $\alpha_{A^+} := A^+(a, a)$  and  $\alpha_{A^-} := A^-(a, a)$  are independent of  $a \in X$ .

**Definitions 2.3** A *refined spin model* is a triple  $(W^+, V^+, d)$  such that

- $(W^+, d)$  is a spin model;
- $V^+$  is a symmetric matrix belonging to the Nomura algebra  $N_W$ ;
- $\alpha_{V^+} \cdot \alpha_{V^-} \neq 0$ .

A *refined spin model of type II* is a refined spin model  $(W^+, V^+, d)$  such that  $V^+$  is a *type II matrix*, i.e., such that  $V^+ \circ V^- = J$ .

**Remark 2.4** Every spin model  $(W^+, d)$  admits a refinement  $(W^+, V^+, d)$  of type II. Indeed, by definition  $I \in N_W$ , therefore  $J = \psi(I) \in N_W$ . Thus, if  $\xi \in \mathbb{C} \setminus \{0\}$  is one of the four complex numbers such that  $d = -\xi^2 - \xi^{-2}$ , the symmetric type II matrix  $(-\xi^{-3})I + \xi(J - I) \in N_W$  can be chosen as  $V^+$ . In other words, each spin model  $(W^+, d)$  admits four type II refinements of the form  $(W^+, V_{\text{Potts}}^+, d)$ , where  $V_{\text{Potts}}^+ = (-\xi^{-3})I + \xi(J - I)$ . Note that  $(V_{\text{Potts}}^+, d)$  is a Potts model. Refined spin models of the form  $(W^+, V_{\text{Potts}}^+, d)$  will be referred to as *Potts-refined spin models*.

Let  $\widehat{M} = (W^+, V^+, d)$  be a refined spin model,  $D$  an oriented, symmetric link diagram, and  $c$  a chequerboard colouring of  $\mathbb{R}^2 \setminus D$ . Let  $\Gamma_D$  be the planar, signed medial graph associated with the black regions of  $c$ . The set  $\Gamma_D^1$  of the edges of  $\Gamma_D$  contains the set  $\Gamma_B^1$  of edges corresponding to crossings on the axis. We define the

partition function  $Z_{\widehat{M}}(D, c)$  by the formula

$$Z_{\widehat{M}}(D, c) := d^{-N} \sum_{\sigma: \Gamma_D^0 \rightarrow X} \prod_{e \in \Gamma_B^1} V^{s(e)}(\sigma(v_e), \sigma(w_e)) \times \prod_{e \in \Gamma_D^1 \setminus \Gamma_B^1} W^{s(e)}(\sigma(v_e), \sigma(w_e)),$$

where  $s(e) \in \{+, -\}$  is the sign of the edge  $e$ , and the *normalized partition function*  $I_{\widehat{M}}(D, c)$  by  $I_{\widehat{M}}(D, c) := \alpha_{V^+}^{-p_B(D)} \alpha_{V^-}^{-n_B(D)} Z_{\widehat{M}}(D, c)$ , where  $p_B(D)$  and  $n_B(D)$  denote, respectively, the numbers of positive and negative crossings on the axis. As in the case of the ordinary spin models, when  $D$  is not connected we define both  $Z_{\widehat{M}}(D, c)$  and  $I_{\widehat{M}}(D, c)$  as the product of the values of  $Z_{\widehat{M}}$  and, respectively,  $I_{\widehat{M}}$  on its connected components with the induced colourings.

We are ready to state our main result. Its proof will be given in the next section.

**Theorem 2.5** *Let  $\widehat{M}$  be a refined spin model and let  $D_i \subset \mathbb{R}^2$ ,  $i = 1, 2$  be two oriented, symmetrically equivalent symmetric (with respect to the axis  $B$ ) union diagrams. Then, for any choice of checkerboard colourings  $c_i$  of  $\mathbb{R}^2 \setminus D_i$ , we have*

$$(2.5) \quad I_{\widehat{M}}(D_1, c_1) = I_{\widehat{M}}(D_2, c_2).$$

Moreover, if  $\widehat{M}$  is of type II, then (2.5) holds if  $D_1$  and  $D_2$  are weakly symmetrically equivalent.

### 3 Proof of Theorem 2.5

Throughout Section 3 we denote by  $\widehat{M}$  a fixed refined spin model  $(W^+, V^+, d)$  and by  $M$ , its underlying spin model  $(W^+, d)$ .

#### 3.1 Invariance Under the $sR$ and the $S2(h)$ Moves

**Proposition 3.1** *Let  $\widehat{M}$  be a refined spin model and  $(D, c)$  and  $(D', c')$  two coloured and oriented symmetric link diagrams. If  $(D', c')$  is obtained from  $(D, c)$  by applying either an  $S2(h)$  move or a symmetric Reidemeister move off the axis, then  $I_{\widehat{M}}(D, c) = I_{\widehat{M}}(D', c')$ .*

**Proof** An  $S2(h)$ -move does not change the edges of the medial graph  $\Gamma_D$  corresponding to crossings on the axis. Therefore the equality  $I_{\widehat{M}}(D', c') = I_{\widehat{M}}(D, c)$  holds for the same reason as the equality  $I_M(D) = I_M(D')$  [1,6]. A similar argument applies for a symmetric Reidemeister move off the axis. ■

#### 3.2 Invariance Under the $S3$ and the $S2(\pm)$ Moves

Suppose that the medial graphs  $\Gamma_D$  and  $\Gamma_{D'}$  of two coloured, oriented, symmetric link diagrams  $(D, c)$  and  $(D', c')$  appear locally as in Figure 6 and coincide elsewhere. The dashed arrows represent edges corresponding to crossings on the axis; let us ignore the vertex labels for the moment. Then we claim that the equality  $I_{\widehat{M}}(D, c) = I_{\widehat{M}}(D', c')$  holds for each refined spin model  $\widehat{M}$ . As explained in Subsection 2.1, we have  $\psi(V^+) = dV^-$  if and only if  $V^+ Y_{ab}^{W^+} = dV^-(a, b) Y_{ab}^{W^+}$  for every  $a, b \in X$ .



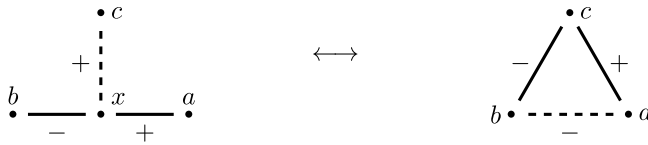


Figure 6: The directed medial graphs  $\Gamma_D$  (left) and  $\Gamma_{D'}$  (right).

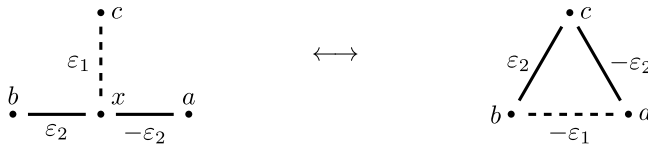


Figure 7: All the star-triangle identities in graphical form.

More explicitly, for each  $a, b, c \in X$

$$(3.1) \quad \sum_{x \in X} V^+(x, c)W^+(x, a)W^-(b, x) = dV^-(a, b)W^+(c, a)W^-(b, c).$$

As the labels in Figure 6 show, equation (3.1) guarantees that the different local contributions to the normalized partition functions for  $D$  and  $D'$  coincide. Note that, although the three vertices labelled  $a, b$ , and  $c$  are drawn as if they were distinct, the equality  $I_{\widehat{M}}(D, c) = I_{\widehat{M}}(D', c')$  still holds if two of them coincide.

All possible instances of locally different medial graphs with the same normalized partition functions are displayed in Figure 7, where  $\varepsilon_1, \varepsilon_2 \in \{\pm\}$ . We will make use of them in Subsections 3.2 and 3.4. The previous remark about the vertices labelled  $a, b$ , and  $c$  applies. Following standard terminology, we shall call *star-triangle identities* the identities in Figure 7. The reason why such identities hold is the following. As explained in Subsection 2.2, the equality  $\psi(V^+) = dV^-$  implies that  $\psi(V^-) = dV^+$ , which is equivalent to saying that  $V^-Y_{ab}^{W^+} = dV^+(a, b)Y_{ab}^{W^+}$  for every  $a, b \in X$ . Moreover, since  $Y_{ab}^{W^+} = Y_{ba}^{W^-}$  for every  $a, b \in X$ , we also have  $V^+Y_{ab}^{W^-} = dV^-(a, b)Y_{ab}^{W^-}$  and  $V^-Y_{ab}^{W^-} = dV^+(a, b)Y_{ab}^{W^-}$  for every  $a, b \in X$ . One can now easily check that these equations imply the identities of Figure 7.

The following remark will be used in Subsection 3.4.

**Remark 3.2** The algebraic identities represented by the graphs of Figure 7 hold for the normalized partition function (defined in the obvious way) of any signed graph  $\Gamma$  with some distinguished edges. In particular,  $\Gamma$  does not need to be the medial graph of a diagram transverse to the axis.

**Proposition 3.3** Let  $\widehat{M}$  be a refined spin model and  $(D, c), (D', c')$  two coloured, oriented symmetric union link diagrams. If  $(D', c')$  is obtained from  $(D, c)$  by applying a symmetric Reidemeister move of type  $S3(o\pm)$  or  $S3(u\pm)$ , then  $I_{\widehat{M}}(D, c) = I_{\widehat{M}}(D', c')$ .

**Proof** The possible local changes of a coloured symmetric union diagram are obtained from the one shown in Figure 8 by mirroring the picture or rotating it by  $180^\circ$

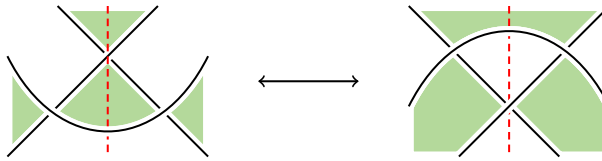


Figure 8: (Colour online) Local changes induced by  $S_3$  moves.

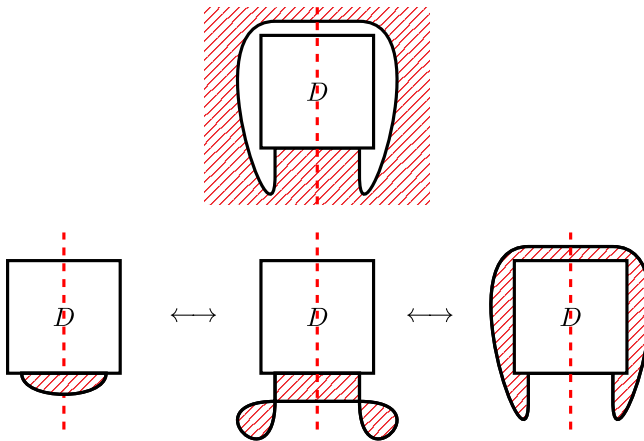


Figure 9: (Colour online) Independence of  $I_{\widehat{M}}$  from the choice of colouring.

around the  $x$ ,  $y$ , or  $z$  axes. It is a straightforward exercise to check that all the changes of the corresponding medial graphs are included among the ones described by Figure 7. This immediately implies the statement. ■

**Corollary 3.4** *Let  $\widehat{M}$  be a refined spin model and  $D$  an oriented, symmetric union link diagram. Given distinct colourings  $c$  and  $c'$ , we have*

$$I_{\widehat{M}}(D, c) = I_{\widehat{M}}(D, c').$$

**Proof** The proof we give is similar in spirit to the proof of [6, Proposition 2.14]. Since  $D$  is a symmetric union diagram, at least one strand of  $D$  intersects the axis away from the crossings. Applying a sequence of symmetric Reidemeister moves,  $S_2(h)$  moves, and  $S_3$  moves, we can shift that strand *downwards* without changing  $I_{\widehat{M}}$ . Hence, we assume without loss of generality that  $(D, c)$  looks like the coloured diagram shown in the bottom left picture in Figure 9. Note that the medial graph of  $(D, c)$  coincides with the medial graph of the top diagram in Figure 9. Another sequence of symmetric Reidemeister moves,  $S_2(h)$  and  $S_3$  moves as suggested in the bottom pictures of Figure 9 turns  $(D, c)$ , without altering  $I_{\widehat{M}}$ , into the bottom right diagram of Figure 9, which has the same medial graph as  $(D, c')$ . ■

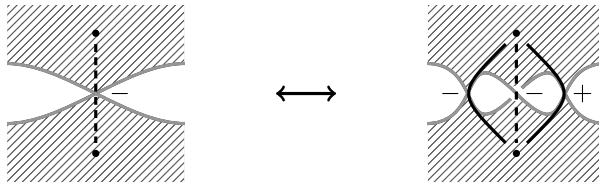


Figure 10: (Colour online) Coloured diagrams and medial graphs differing by an  $S2(-)$  move.

In view of Corollary 3.4, henceforth we shall omit the colouring from the notation for the normalized partition function of symmetric union diagrams.

**Proposition 3.5** *Let  $D$  and  $D'$  be two oriented, symmetric union link diagrams. If  $D'$  is obtained from  $D$  by applying a symmetric Reidemeister move of type  $S2(+)$  or  $S2(-)$ , then  $I_{\widehat{M}}(D') = I_{\widehat{M}}(D)$ .*

**Proof** By Corollary 3.4, it suffices to prove the statement for any choice of colouring. The case of an  $S2(-)$  move is illustrated in Figure 10. The statement follows immediately from equation (2.1). The case of an  $S2(+)$  is similar and left to the reader. ■

### 3.3 Invariance Under the $S1$ Moves

**Proposition 3.6** *Let  $\widehat{M}$  be a refined spin model and let  $D, D'$  be two oriented, symmetric union link diagrams. If  $D'$  is obtained from  $D$  by applying an  $S1$  move, then  $I_{\widehat{M}}(D') = I_{\widehat{M}}(D)$ .*

**Proof** As in the proof of Proposition 3.3, the local change of a symmetric union diagram due to a move of type  $S1(-)$  is given, up to symmetries, by the left-hand portion of Figure 5. In view of Corollary 3.4, the choice of colouring is irrelevant, so we make that choice so that the corresponding local change of medial graphs is the one given by Figure 11. Suppose that  $\Gamma_{D'}$  is locally given by the left-hand side of Figure 11, denote by  $v_0$  the vertex labelled  $a$  and by  $e_0$  the dashed edge connecting  $v_0$  to the vertex labelled  $x$ . Let  $N = |\Gamma_D^0|$  be the number of vertices of  $\Gamma_D$  so that  $|\Gamma_{D'}^0| = N + 1$ . By the definition of the partition function we have

$$\begin{aligned} Z_{\widehat{M}}(D') &= d^{-N-1} \sum_{\sigma: \Gamma_{D'}^0 \rightarrow X} \prod_{e \in \Gamma_B^1} V^{s(e)}(\sigma(v_e), \sigma(w_e)) \\ &\quad \times \prod_{e \in \Gamma_{D'}^1 \setminus \Gamma_B^1} W^{s(e)}(\sigma(v_e), \sigma(w_e)) \\ &= d^{-N} \sum_{\sigma: \Gamma_D^0 \rightarrow X} \left[ \frac{1}{d} \sum_{x \in X} V^+(\sigma(v_0), x) \right] \prod_{e \in \Gamma_B^1 \setminus \{e_0\}} V^{s(e)}(\sigma(v_e), \sigma(w_e)) \\ &\quad \times \prod_{e \in \Gamma_D^1 \setminus \Gamma_B^1} W^{s(e)}(\sigma(v_e), \sigma(w_e)) \\ &= \alpha_{V-} Z_{\widehat{M}}(D), \end{aligned}$$

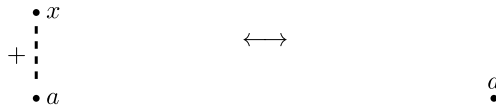


Figure 11: Local change due to an S1 move.

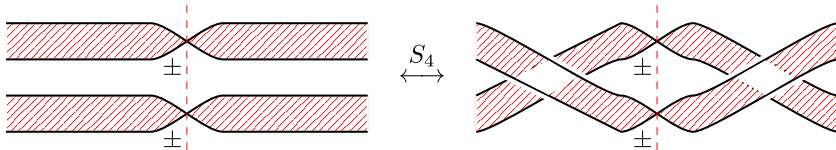


Figure 12: (Colour online) The choice of colouring for the S4 move.

where the last equality is due to the fact that  $\frac{1}{d} \sum_{x \in X} V^+(a, x) = \alpha_{V^-}$  for each  $a \in X$ , which follows from (2.4). The equality  $I_{\widehat{M}}(D') = I_{\widehat{M}}(D)$  now follows immediately from  $p_B(D') = p_B(D)$  and  $n_B(D') = n_B(D) + 1$ . The argument for an S1(+) move is similar and left to the reader. ■

### 3.4 Invariance Under the S4 Moves

In view of the results of Subsections 3.1, 3.2, and 3.3, the following concludes the proof of the first part of Theorem 2.5.

**Proposition 3.7** *Let  $\widehat{M}$  be a refined spin model, and let  $D, D'$  be two oriented, symmetric union link diagrams. If  $D'$  is obtained from  $D$  by applying an S4 move, then  $I_{\widehat{M}}(D') = I_{\widehat{M}}(D)$ .*

**Proof** By Corollary 3.4 we can choose an arbitrary colouring. We choose the configuration of Figure 12. There are a number of possible cases, depending on the types of crossings on the axis and whether the two top strands go over or under the two bottom strands. As illustrated in Figure 12, we now consider all configurations of crossings on the axis simultaneously and we assume that the two top strands go over the two bottom strands. It is easy to check that the graphs  $\Gamma_1$  and  $\Gamma_2$  associated with the diagrams of Figure 12 are locally as in Figure 13, where  $\varepsilon_1, \varepsilon_2 \in \{+, -\}$ . As we now explain, Figure 14 contains the proof that the graphs  $\Gamma_1$  and  $\Gamma_2$  have equal invariants  $I_{\widehat{M}}$ . Indeed, the upper part of Figure 14 describes the application to  $\Gamma_2$  of two star-triangle identities from Figure 7, resulting in the graph  $\Gamma'_2$ . Note that, in view of Remark 3.2, we do not need to keep track of the axis but only of the graphs and their distinguished edges. Equation (2.1) allows us to cancel the two edges of  $\Gamma'_2$  connecting the vertices  $t$  and  $y$ , obtaining the graph  $\Gamma''_2$ . The lower part of Figure 14 shows how two more star-triangle identities can be applied to  $\Gamma''_2$  to obtain the graph  $\Gamma'_1$ . After two more edge cancellations we get graph  $\Gamma_1$ . Observe that the vertices labelled  $a$  and  $b$ , as well as those labelled  $c$  and  $d$ , are drawn as if they were distinct, but the proof goes through

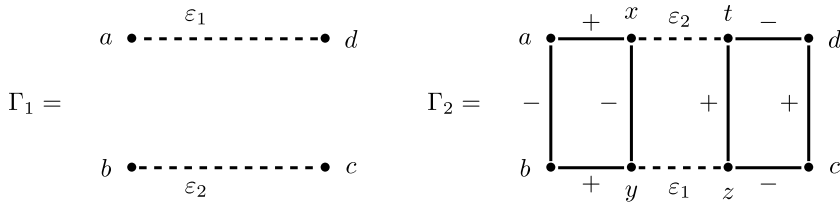


Figure 13: Local change of the medial graph under an S4 move.

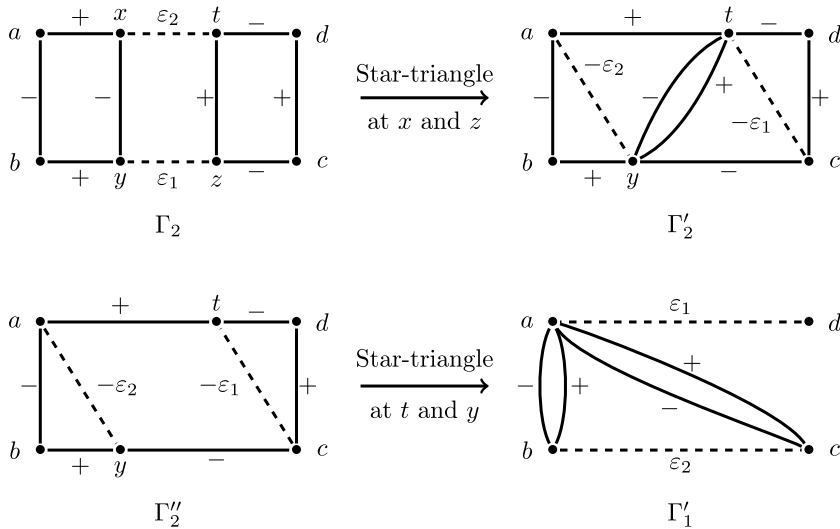


Figure 14: Invariance of  $I_{\widehat{M}}$  under the S4 move.

if they coincide. This concludes the argument in the cases when the two top strands go over the two bottom strands. The argument for the other cases is essentially the same, and therefore omitted. ■

### 3.5 Invariance Under the $S2(v)$ Moves

The following result concludes the proof of the second part of Theorem 2.5.

**Proposition 3.8** *Let  $\widehat{M}$  be a refined spin model of type II and let  $D, D'$  be two oriented, symmetric union link diagrams. If  $D'$  is obtained from  $D$  by applying an  $S2(v)$  move, then  $I_{\widehat{M}}(D') = I_{\widehat{M}}(D)$ .*

**Proof** The proof is very simple. Suppose that  $D$  and  $D'$  are the diagrams shown on the right-hand side of Figure 5, with  $D'$  having two more crossings on the axis. It is clear that we can choose the colourings so that  $\Gamma_{D'}^0 = \Gamma_D^0$  and  $\Gamma_{D'}$  has two more edges on the axis with opposite signs, connecting the same two vertices. The fact that  $\widehat{M}$  is

of type II implies that  $Z_{\widehat{M}}(D') = Z_{\widehat{M}}(D)$  and the fact that the two extra crossings of  $D'$  have opposite signs gives  $I_{\widehat{M}}(D') = I_{\widehat{M}}(D)$ . ■

## 4 Applications

### 4.1 Refined Potts Models and the $10_{42}$ Diagrams

Consider a Potts model  $M = (W_{\text{Potts}}^+, d)$  as in Example 2.11 for  $n = 3$ . Recall that  $W_{\text{Potts}}^+ = (-\xi^{-3})I + \xi(J - I)$ , where  $d = -\sqrt{3} = -\xi^2 - \xi^{-2}$ . By Remark 2.4 we have  $I, J \in N_W$ . Therefore, any matrix of the form  $V_{a,b}^+ = aI + b(J - I)$ ,  $a, b \in \mathbb{C}$  is symmetric and belongs to  $N_W$ . Since  $\psi(I) = J$  and therefore  $\psi(J) = \psi^2(I) = nI$ , we have

$$\Psi(V_{a,b}^+) = (a + 2b)I + (a - b)(J - I) = dV^-.$$

Hence, if  $a(a + 2b) \neq 0$ , we have a refined spin model of the form  $\widehat{M}_{a,b} = (W_{\text{Potts}}^+, V_{a,b}^+, d)$ . Let  $D_{10_{42}}$  (respectively,  $D'_{10_{42}}$ ) be the central (respectively, right-most) symmetric union diagram of Figure 4. A Sage [9] computation gives

$$I_{\widehat{M}_{a,b}}(D_{10_{42}}) = d \frac{a^3 + 6a^2b + 2b^3}{a(a + 2b)^2} \quad \text{and} \quad I_{\widehat{M}_{a,b}}(D'_{10_{42}}) = d \frac{3a}{a + 2b}.$$

Clearly, for infinitely many choices of  $(a, b)$  with  $a(a + 2b) \neq 0$ , we have

$$I_{\widehat{M}_{a,b}}(D_{10_{42}}) \neq I_{\widehat{M}_{a,b}}(D'_{10_{42}}),$$

and, applying Theorem 2.5, we conclude that  $D_{10_{42}}$  and  $D'_{10_{42}}$  are not symmetrically equivalent. This gives a partial answer to the question left open by Eisermann and Lamm and described at the end of Subsection 1.2.<sup>2</sup>

### 4.2 Refined Pentagonal Models and the $8_9$ Diagrams

Now we consider the pentagonal spin model of Example 2.12. We want to define a refined spin model of the form  $\widehat{M}_{\text{pent}} = (W_{\text{pent}}^+, V^+, d)$ , where

$$W_{\text{pent}}^+ = I + \omega A_1 + \omega^4 A_2, \quad \omega = e^{2\pi i/5}, \quad d = \sqrt{5}$$

and

$$A_1 = \begin{pmatrix} 0 & 1 & 0 & 0 & 1 \\ 1 & 0 & 1 & 0 & 0 \\ 0 & 1 & 0 & 1 & 0 \\ 0 & 0 & 1 & 0 & 1 \\ 1 & 0 & 0 & 1 & 0 \end{pmatrix}, \quad A_2 = \begin{pmatrix} 0 & 0 & 1 & 1 & 0 \\ 0 & 0 & 0 & 1 & 1 \\ 1 & 0 & 0 & 0 & 1 \\ 1 & 1 & 0 & 0 & 0 \\ 0 & 1 & 1 & 0 & 0 \end{pmatrix}.$$

It is easy to check that both  $A_1$  and  $A_2$  belong to the Nomura algebra  $N_W$ . If we let  $V^+ = aI + bA_1 + cA_2 \in N_W$ , we need to check for which  $a, b, c \in \mathbb{C}$  we have  $\alpha_{V^+} \cdot \alpha_{V^-} \neq 0$ . Clearly  $\alpha_{V^+} = a$  and, since  $V^+ Y_{aa}^{W^+} = a + 2b + 2c$ , we have  $\alpha_{V^-} = (a + 2b + 2c)/d$ .

<sup>2</sup>All the refined spin models of type II that we were able to use had normalized partition functions that took the same values on  $D_{10_{42}}$  and  $D'_{10_{42}}$ . However, we do not know how relevant this information is for the question whether  $D_{10_{42}}$  and  $D'_{10_{42}}$  are weakly symmetrically equivalent. In fact, on the one hand, we could not perform a large amount of calculations because their intensity grew very quickly with the size of model. On the other hand, at the time of writing there is no general classification of spin models; therefore some newly discovered spin model could work in the future.

Therefore,  $\widehat{M}_{\text{pent}} = (W_{\text{pent}}^+, V^+, d)$  is a refined spin model for every  $a, b, c \in \mathbb{C}$  such that  $a(a + 2b + 2c) \neq 0$ . Let  $D_{8_9}$  be the left-most diagram of Figure 4 and  $D'_{8_9}$  the diagram obtained from  $D_{8_9}$  by switching all the crossings on the axis. A computation with Sage [9] yields

$$I_{\widehat{M}_{\text{pent}}}(D_{8_9}) = d[a(a^2 + 2ab + 2ac + 2b^2 + 2c^2) + (d - 1)(b^3 + c^3) - (d + 1)bc(b + c)]/a^2(a + 2b + 2c)$$

and

$$I_{\widehat{M}_{\text{pent}}}(D'_{8_9}) = d[a^2(a + 6b + 6c) + 2(d + 1)a(b^2 + c^2) + (3 - d)(b^3 + c^3) + 4(1 - d)abc + (d - 1)bc(b + c)]/a(a + 2b + 2c)^2.$$

In particular,

$$I_{\widehat{M}_{\text{pent}}}(D_{8_9})_{a=1, c=-b} = d(4b^2 + 1) \neq I_{\widehat{M}_{\text{pent}}}(D'_{8_9})_{a=1, c=-b} = 40b^2 + d,$$

which, by Theorem 2.5, implies that the diagrams  $D_{8_9}$  and  $D'_{8_9}$  are not symmetrically equivalent. In fact, if we choose  $\xi \in \mathbb{C}$  such that  $\xi^2 = (1 - d)/2$  and we set  $b = c = \xi \in \mathbb{C}$  and  $a = -\xi^{-3}$ , we have  $d = -\xi^2 - \xi^{-2}$  and we obtain a Potts-refined spin model (see Remark 2.4). Substituting these values of  $a, b$ , and  $c$  we get

$$I_{\widehat{M}_{\text{pent}}}(D_{8_9})_{a=-\xi^{-3}, b=c=\xi} = -5d + 10 \neq I_{\widehat{M}_{\text{pent}}}(D'_{8_9})_{a=-\xi^{-3}, b=c=\xi} = -5d - 10.$$

This shows that  $D_{8_9}$  and  $D'_{8_9}$  are not weakly symmetrically equivalent.

### 4.3 Infinitely Many Symmetrically Inequivalent Diagrams

Eisermann and Lamm [2, §2.5] defined the connected sum between two symmetric union diagrams  $D$  and  $D'$  by putting  $D$  above  $D'$  along the axis  $B$  and then symmetrically joining a strand of  $D$  transverse to  $B$  to a strand of  $D'$  transverse to  $B$ . They showed that this results in an associative operation that is well defined on weakly symmetric equivalence classes and denoted the connected sum of the symmetric union diagrams  $D$  and  $D'$  by  $D\#D'$ . Up to applying  $S3$  and  $S2(h)$  moves, one may always assume that the strands of  $D$  or  $D'$  used for the operation are, respectively, at the very bottom of  $D$  and at the very top of  $D'$  (see [2, Figure 17]). Proposition 4.1 below, whose proof will be provided in Section 5, allows us to establish Theorem 4.2 below, which easily implies the existence of infinitely many pairs of symmetrically inequivalent, but Reidemeister equivalent symmetric union diagrams.

We need one more definition before we can state Proposition 4.1. View a complex  $n \times n$  matrix  $A \in \text{Mat}_X(\mathbb{C})$  as a map  $A: X \times X \rightarrow \mathbb{C}$  with  $X = \{1, \dots, n\}$ , and let  $t: X \rightarrow X$  be the shift map given by  $t(a) = a + 1 \pmod n$  for each  $a \in X$ . We say that a refined spin model  $\widehat{M} = (W^+, V^+, d)$  is *translation-invariant* if

$$W^\pm(t(a), t(b)) = W^\pm(a, b) \quad \text{and} \quad V^\pm(t(a), t(b)) = V^\pm(a, b)$$

for each  $a, b \in X$ .

**Proposition 4.1** *Let  $\widehat{M}$  be a translation-invariant, refined spin model and let  $D, D_1$ , and  $D_2$  be oriented, symmetric union link diagrams. Suppose that  $\Gamma_D = \Gamma_{D_1} \cup \Gamma_{D_2}$ ,*

where  $\Gamma_{D_1}$  and  $\Gamma_{D_2}$  are subgraphs of  $\Gamma_D$  intersecting in a single vertex  $v_0$ . Then  $I_{\widehat{M}}(D) = \frac{1}{d} I_{\widehat{M}}(D_1) I_{\widehat{M}}(D_2)$ .

**Theorem 4.2** *Let  $D, D'$  be Reidemeister equivalent, oriented symmetric union link diagrams. If  $I_{\widehat{M}}(D) \neq I_{\widehat{M}}(D')$  for some translation-invariant refined spin model  $\widehat{M}$ , then for infinitely many  $k \geq 1$  the connected sums*

$$\#^k D = D \# \overset{(k \text{ times})}{\dots} \# D \quad \text{and} \quad \#^k D' = D' \# \overset{(k \text{ times})}{\dots} \# D'$$

*are Reidemeister equivalent, but not symmetrically equivalent. If  $\widehat{M}$  is of type II, then  $\#^k D$  and  $\#^k D'$  are not weakly symmetrically equivalent. Moreover, the same conclusions hold for each  $k \geq 1$  if either  $I_{\widehat{M}}(D) = \lambda I_{\widehat{M}}(D')$  or  $I_{\widehat{M}}(D') = \lambda I_{\widehat{M}}(D)$ , where  $\lambda \in \mathbb{R}_{\geq 0}$ .*

**Proof** Proposition 4.1 applies to triples of the form  $D = D_1 \# D_2$ ,  $D_1, D_2$ , where the connected sum is performed using a bottom transverse strand of  $D_1$  and a top transverse strand of  $D_2$ , as explained above. Hence, for each  $k \geq 1$  we have

$$I_{\widehat{M}}(\#^k D) = \frac{1}{d^{k-1}} I_{\widehat{M}}(D)^k, \quad \text{and} \quad I_{\widehat{M}}(\#^k D') = \frac{1}{d^{k-1}} I_{\widehat{M}}(D')^k.$$

Therefore, the equality  $I_{\widehat{M}}(\#^k D) = I_{\widehat{M}}(\#^k D')$  implies  $I_{\widehat{M}}(D) = \zeta I_{\widehat{M}}(D')$  with  $\zeta^k = 1$ , and the statement follows easily. ■

**Corollary 4.3** *Let  $D_{10_{42}}, D'_{10_{42}}, D_{8_9}$ , and  $D'_{8_9}$  be the symmetric union diagrams considered in Subsections 4.1 and 4.2. Then, for each  $k \geq 1$ , the symmetric union diagrams  $\#^k D_{10_{42}}$  and  $\#^k D'_{10_{42}}$  are Reidemeister equivalent, but not symmetrically equivalent, while  $\#^k D_{8_9}$  and  $\#^k D'_{8_9}$  are Reidemeister, but not weakly symmetrically equivalent.*

**Proof** Let  $\widehat{M}_{a,b}$  be the refined spin model defined in Subsection 4.1. By the calculations given there we have

$$I_{\widehat{M}_{1,0}}(D_{10_{42}}) = -\sqrt{3} \quad \text{and} \quad I_{\widehat{M}_{1,0}}(D'_{10_{42}}) = -3\sqrt{3}.$$

Since the Potts model is translation invariant, applying Theorem 4.2 we obtain that, for each  $k \geq 1$ , the diagrams  $\#^k D_{10_{42}}$  and  $\#^k D'_{10_{42}}$  are not symmetrically equivalent. Similarly, by the results of Subsection 4.2, if  $\xi^2 = (1 - \sqrt{5})/2$  we have

$$I_{\widehat{M}_{\text{pent}}}(D_{8_9})_{a=-\xi^{-3}, b=c=\xi} = 10 - 5\sqrt{5},$$

$$I_{\widehat{M}_{\text{pent}}}(D'_{8_9})_{a=-\xi^{-3}, b=c=\xi} = -10 - 5\sqrt{5}.$$

As before, since the pentagonal model is translation invariant, we may apply Theorem 4.2. Therefore, for each  $k \geq 1$  the diagrams  $\#^k D_{8_9}$  and  $\#^k D'_{8_9}$  are not weakly symmetrically equivalent. ■

### 5 Proof of Proposition 4.1

Recall from Section 2 that if  $\widehat{M} = (W^+, V^+, d)$  is a refined spin model, the normalized partition function of a symmetric union diagram  $D$  takes the form

$$I_{\widehat{M}}(D) = \alpha_{V^+}^{-p_B(D)} \alpha_{V^-}^{-n_B(D)} d^{-N} Z_{\widehat{M}}(D),$$



where  $N = |\Gamma_D^0|$  and

$$Z_{\widehat{M}}(D) = d^{-N} \sum_{\sigma: \Gamma_D^0 \rightarrow X} \prod_{e \in \Gamma_B^1} V^{s(e)}(\sigma(v_e), \sigma(w_e)) \prod_{e \in \Gamma_D^1 \setminus \Gamma_B^1} W^{s(e)}(\sigma(v_e), \sigma(w_e)).$$

Here we are omitting the colouring from the notation because of Corollary 3.4. Fix a vertex  $v_0 \in \Gamma_D^0$  and an element  $a \in X$ . Define

$$R_{\widehat{M}}(D, v_0; a) := \sum_{\sigma | \sigma(v_0) = a} \prod_{e \in \Gamma_B^1} V^{s(e)}(\sigma(v_e), \sigma(w_e)) \times \prod_{e \in \Gamma_D^1 \setminus \Gamma_B^1} W^{s(e)}(\sigma(v_e), \sigma(w_e)).$$

Then we have  $Z_{\widehat{M}}(D) = d^{-N} \sum_{a \in X} R_{\widehat{M}}(D, v_0; a)$ .

**Lemma 5.1** *If  $\widehat{M} = (W^+, V^+, d)$  is a translation-invariant refined spin model,  $Z_{\widehat{M}}(D) = nd^{-N} R_{\widehat{M}}(D, v_0; a)$  for each  $v_0 \in \Gamma_D^0$  and  $a \in X$ .*

**Proof** It suffices to show that  $R_{\widehat{M}}(D, v_0; a) = R_{\widehat{M}}(D, v_0; t(a))$  for each  $a \in X$ , where  $t(a) = a + 1 \pmod n$ . Let

$$w(\sigma, e) = \begin{cases} W^{s(e)}(\sigma(v_e), \sigma(w_e)) & \text{if } e \text{ is off the axis,} \\ V^{s(e)}(\sigma(v_e), \sigma(w_e)) & \text{if } e \text{ is on the axis,} \end{cases}$$

where  $s(e) \in \{+, -\}$  is the sign of  $e$ . Since the spin model is translation-invariant,

$$\sum_{\sigma | \sigma(v_0) = a} \prod_e w(\sigma, e) = \sum_{\sigma | t \circ \sigma(v_0) = t(a)} \prod_e w(t \circ \sigma, e) = \sum_{\sigma | \sigma(v_0) = t(a)} \prod_e w(\sigma, e),$$

which implies the required identity. ■

Clearly  $R_{\widehat{M}}(D, v_0; a) = R_{\widehat{M}}(D_1, v_0; a) R_{\widehat{M}}(D_2, v_0; a)$  for each  $a \in X$ . Let  $N = |\Gamma_D^0|$ ,  $N_1 = |\Gamma_{D_1}^0|$ , and  $N_2 = |\Gamma_{D_2}^0|$ . Then we have  $N = N_1 + N_2 - 1$ . Now choose any  $x_0 \in X$ . Since  $d^2 = n$ ,  $p_B(D) = p_B(D_1) + p_B(D_2)$ , and  $n_B(D) = n_B(D_1) + n_B(D_2)$ , in view of Lemma 5.1 we have

$$\begin{aligned} dI_{\widehat{M}}(D) &= \alpha_{V^+}^{-p_B(D)} \alpha_{V^-}^{-n_B(D)} d^{-N+1} Z_{\widehat{M}}(D) \\ &= n_B I_{V^+}^{-p_B(D)} \alpha_{V^-}^{-n_B(D)} d^{-N+1} R_{\widehat{M}}(D, v_0; x_0) \\ &= d^{-N_1} \alpha_{V^+}^{-p_B(D_1)} \alpha_{V^-}^{-n_B(D_1)} n R_{\widehat{M}}(D_1, v_0; x_0) \\ &\quad \times d^{-N_2} \alpha_{V^+}^{-p_B(D_2)} \alpha_{V^-}^{-n_B(D_2)} n R_{\widehat{M}}(D_2, v_0; x_0) \\ &= I_{\widehat{M}}(D_1) I_{\widehat{M}}(D_2). \end{aligned}$$

This concludes the proof of Proposition 4.1.

**Acknowledgements** Author C.C. wishes to thank Francesco Costantino and the IMT for their hospitality. The authors are grateful to the anonymous referee for helpful comments and suggestions.

## References

- [1] Pierre de la Harpe, *Spin models for link polynomials, strongly regular graphs and Jaeger's Higman-Sims model*. Pacific J. Math. 162(1994), no. 1, 57–96.
- [2] Michael Eisermann and Christoph Lamm, *Equivalence of symmetric union diagrams*. J. Knot Theory Ramifications 16(2007), no. 07, 879–898. <https://doi.org/10.1142/S0218216507005555>.
- [3] Michael Eisermann and Christoph Lamm, *A refined Jones polynomial for symmetric unions*. Osaka J. Math. 48(2011), no. 2, 333–370.
- [4] David M. Goldschmidt and Vaughan F. R. Jones, *Metaplectic link invariants*. Geom. Dedicata 31(1989), no. 2, 165–191. <https://doi.org/10.1007/BF00147477>.
- [5] François Jaeger, Makoto Matsumoto, and Kazumasa Nomura, *Bose-Mesner Algebras Related to Type II Matrices and Spin Models*. J. Algebraic Combin. 8(1998), no. 1, 39–72. <https://doi.org/10.1023/A:1008691327727>.
- [6] Vaughan Jones, *On knot invariants related to some statistical mechanical models*. Pacific J. Math. 137(1989), no. 2, 311–334.
- [7] Vaughan F. R. Jones, *On a certain value of the Kauffman polynomial*. Commun. Math. Phys. 125(1989), no. 3, 459–467.
- [8] Kazumasa Nomura, *An algebra associated with a spin model*. J. Algebraic Combin. 6(1997), no. 1, 53–58. <https://doi.org/10.1023/A:1008644201287>.
- [9] The Sage Developers, SageMath, the Sage Mathematics Software System (Version 8.0), <http://www.sagemath.org> (2017).

*Mathematical Sciences, Durham University, UK*

*e-mail:* [carlo.collari.math@gmail.com](mailto:carlo.collari.math@gmail.com)

*Department of Mathematics, University of Pisa, Italy*

*e-mail:* [paolo.lisca@unipi.it](mailto:paolo.lisca@unipi.it)